Proceedings of the 17th World Congress
The International Federation of Automatic Control
Seoul, Korea, July 6-11, 2008

Aircraft Automatic Maneouvering System Using Energy-based Control Technique

Lim Jen Nee Jones * **Rini Akmeliawati** ** **Chee Pin Tan** ***

* *Monash University Sunway Campus, 46150 Bandar Sunway, Selangor, Malaysia (e-mail: lim.jen.nee@eng.monash.edu.my)*
** *Dept. Mechatronics Engineering, International Islamic University Malaysia, 53100 Gombak, Selangor, Malaysia (e-mail: rakmelia@ieee.org)*
*** *Monash University Sunway Campus, 46150 Bandar Sunway, Selangor, Malaysia (e-mail: tan.chee.pin@eng.monash.edu.my)*

Abstract: Automatic control systems are implemented in aircraft systems as it contributes to improve flight safety due to minimal routine pilot interaction. In classical aircraft control systems, overlaps in control systems often reduce the efficiency and effectiveness of the overall control of the aircraft. An integrated (robust) controller becomes a necessity especially where the stability and performance robustness are top priorities, process dynamics are known and variation ranges for uncertainties can be estimated. The success in implementing a nonlinear controller using the Nonlinear Energy Method (NEM) in the longitudinal dynamics of the aircraft has surfaced the need to design the lateral controllers and its integration to the entire aircraft control system. In this paper, a lateral controller that provides tracking of given roll and yaw commands is proposed. The controller is based on NEM. The proposed controller is applied to an aircraft model developed by Group of Aeronautical Research and Technology in Europe (GARTEUR) called the Research Civil Aircraft Model (RCAM). The robustness and disturbance rejection of the NEM controller is tested. The closed-loop responses of the aircraft in 'extreme' flight conditions and the presence of parameter variations indicate that the proposed controller can guarantee stability and performance robustness of the aircraft.

Keywords: Nonlinear System Control; Regulation; Tracking; Disturbance Rejection.

1. INTRODUCTION

The implementation of automatic control systems of aircraft has improved safety as described by Lambregts [1998]. Aircraft control systems are not subjected to fatigue and emotion, as compared to the human pilot. The aircraft is protected from basic failure conditions as most automatic control modes come with some form of failure detection. However, overlaps in control systems often reduce the efficiency and effectiveness of the overall control of the aircraft. For example, as mentioned in Lambregts [1998], there are lateral control mode overlaps in classical aircraft control systems. Lambregts [1998] further highlights that the traditional single-input-single-output (SISO) lateral directional control system designs are highly customized, costly and most parts are not reusable as each mode is developed separately. Therefore, there is a need for a generalized reusable multi-input-multi-output (MIMO) design concept which will reduce the complexity of the control and an integrated control, which can minimize the overlaps and increase the efficiency and the effectiveness of the overall control.

A survey of recent work presented in Wahi et al. [18-20 March 2001] shows that the Proportional-Integral-Derivative (PID) control technique was most popular in the industry, including in flight control systems (FCS). This is mainly because it is simple and easy to implement in both hardware and software. However, the PID works best only for processes that are linear and time-invariant. In the case of FCS, gain-scheduling is used. It can be seen that throughout the history of flight control systems, a variety of controllers, such as adaptive control, H_∞ were studied and some of which have been implemented in the fighter aircraft, as presented by Hyde [2000]. Most of this control techniques use aircraft linearized model. On most current aircraft, specific functions such as roll and yaw stabilization are all designed as separate subsystems. See Griswold [2000].

In this paper, we propose a nonlinear energy-based control method (NEM) to track certain roll and yaw commands and at the same time provide roll and yaw stabilization. This control technique is based on passivity based control (PBC) technique, whereby the controller is obtained by modifying the energy-like function(s) of the system's dynamics and damping injection to ensure passivity, as discussed in Ortega et al. [1998]. The proposed controller uses a nonlinear aircraft model. Thus, the nonlinearity in the dynamical equations can be utilized to provide better control. In this paper our proposed controller is applied to handle turning at horizontal plane of a twin engine research civil aircraft model (RCAM) developed by GARTEUR in FM [AG08]. Thus, the aircraft lateral dynamics would be the main focus. Initial work on application of

NEM in aircraft control can be found in Akmeliawati and Mareels [1999], Akmeliawati and Mareels [2001] and Akmeliawati [2001], whereby the technique has successfully integrated flight and propulsion control and shown very good responses for automatic landing with various flight conditions.

This paper is organized as follows. Section 2 provides the design process of the controller for maneuvering flight. In Section 3 a disturbance and robustness analysis of the resulting control laws is presented. Section 4 concludes.

2. NONLINEAR ENERGY-BASED CONTROL METHOD

In designing our controller we have the following control objectives:

- To provide automatic roll and yaw stabilization during manoeuvering.
- To achieve automatic tracking of roll and yaw reference trajectory.

The controller design can be divided into four stages.

- **Energy-based modeling of aircraft dynamics**
  The aircraft (lateral) dynamics are described using the Euler-Lagrange (EL) formalism.
- **Controller design**
  The control laws are developed based on passivity principle, Lyapunov and Invariant Set Theorems.
- **Tuning**
  The controller gains are tuned to satisfy the design criteria.
- **Disturbance rejection and robustness analysis**
  The controller performance is tested against various flight conditions. In this case we perform 12 sets of simulations to provide information on the controller robustness against parameter variations (aircraft mass and CoG position), and dynamical disturbances, such as turbulence and constant side wind.

2.1 Flight trajectory

A trajectory was designed to provide a reference or command value for roll and yaw angles. This trajectory commands the aircraft to make two turns, to an s-shape turn within a total simulation time of 100 seconds at horizontal plane. Fig. 1 gives a graphical representation of the trajectory on the x-y plane of the earth reference axes. In Segment (ii), the aircraft is required to turn left in 30 seconds with a standard $3^o/s$ turn rate. This segment is similar to the trajectory described as Segment (II) of FM [AG08]. An extended version of this turn is added to the trajectory where the aircraft will then turn right at $3^o/s$ turn rate in Segment (iii) so that the aircraft is heading toward the same initial direction, as though it has just changed to a different track that is parallel to the initial track. Table 1 summarizes each segment of the trajectory.

2.2 Performance and Safety Criteria

A set of evaluation criteria to test the performance of the RCAM is described in FM [AG08] where only relevant criteria for the roll and yaw tracking are presented here.

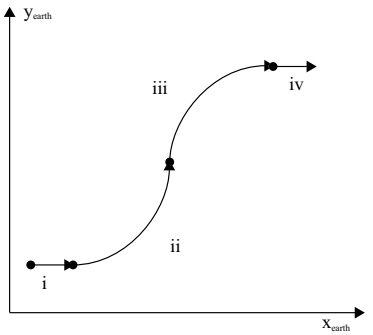

Fig. 1. Flight trajectory

Table 1. Description of Trajectory Segments

Simulation Time	Description
$0s \leq i < 10$s	*Straight*
$10s \leq ii < 40$s	*Left turn at* $3^o/s$
$40s \leq iii < 70$s	*Right turn at* $3^o/s$
$70s \leq iv \leq 100s$	*Straight*

The roll angle steady state deviation should not exceed 5^o and at any time, it should not exceed 30^o for safety reasons. As for the heading angle response, the criteria are as follows:

- The commanded yaw angle, ψ_d, should be tracked by the actual yaw angle, ψ, with a rise time of less than 10 seconds. Rise time here is defined as the time it takes from the response at 10% to 90% of the reference value.
- Settling time of less than 30 seconds to achieve 99% of its final value.
- There should be very little overshoot (less than 5%) in the response to unit steps in commands at altitudes above 305 m but at lower altitudes, overshoot may increase to 30% in order to obtain higher tracking performance.

Most of the criteria set in FM [AG08] are based on a unit step command since classical (linear) controllers are still widely used. As for a nonlinear controllers, these criteria were interpreted to ensure tracking is done by measuring the root-mean-square (RMS) error for the yaw and roll commands.

2.3 Energy-based modeling of aircraft dynamics

Lateral dynamics consists of the translational dynamics (side motion) and the rotational dynamics (roll and yaw). In performing manoeuvering at horizontal plane, the aircraft needs to achieve the reference roll and yaw angles. This involves the coordination of the thrust and the aileron and the rudder deflections.

The detailed mathematical model of RCAM can be found in FM [AG08]. As the scope of this paper covers only the lateral dynamics, two control inputs are fed into the RCAM as specified in Table 2. Other inputs which generally affects the longitudinal dynamics of RCAM are set to its equilibrium points for a flight condition of 80 m/s airspeed. The RCAM outputs listed in Table 3 are used as feedback to the lateral controllers.

Table 2. RCAM input definitions

Inputs	Symbol	Units
Aileron deflection	δ_a	rad
Rudder deflection	δ_r	rad

Table 3. RCAM output definitions

Outputs	Symbol	Units
Roll angle	ϕ	rad
Yaw angle	ψ	rad
Roll rate	$\dot{\phi}$	rad/s
Yaw rate	$\dot{\psi}$	rad/s
Airspeed	V_A	m/s
Pitch angle	θ	rad
Angle of attack	α	rad
Sideslip angle	β	rad

A dynamical system can be defined by an EL equation with n degrees of freedom, with generalized coordinates $q \in R^n$ and external forces $Q \in R^n$

$$\frac{d}{dt}\left(\frac{\partial L}{\partial \dot{q}(q,\dot{q})}\right) - \frac{\partial L}{\partial q}(q,\dot{q}) = Q \tag{1}$$

where

$$L(q,\dot{q}) \triangleq T(q,\dot{q}) - V(q) \tag{2}$$

is the Lagrangian function, $T(q,\dot{q})$ is the kinetic energy function which we assume to be of the form

$$T(q,\dot{q}) = \frac{1}{2}\dot{q}^T D(q)\dot{q}. \tag{3}$$

$D(q) \in R^{n\times n}$ is the generalized inertia matrix that satisfies $D(q) = D^T(q) > 0$ and $V(q)$ is the potential energy function which is assumed to be bounded from below, that is, there exists a $c \in R^n$ such that $V(q) \geq c$ for all $q \in R^n$. The external forces are defined by

$$Q = -\frac{\partial F}{\partial \dot{q}}(\dot{q}) + Q_\zeta + M_u u, \tag{4}$$

where Q_ζ is an external signal that models the effect of disturbances. M_u is the input matrix and u is the input.

An EL system is derived with (5) with n degrees of freedom and generalized coordinates $q \in R^n$ in

$$D(q)\ddot{q} = -\frac{\partial F}{\partial \dot{q}}(\dot{q}) + Q_\zeta + M_u u, \tag{5}$$

where $F(\dot{q})$ is the Rayleigh dissipation function such as aerodynamics forces of the aircraft, which can only be assumed to satisfy

$$\dot{q}^{\mathrm{T}}\frac{\partial F}{\partial \dot{q}}(\dot{q}) \geq 0 \tag{6}$$

at this stage.

The RCAM can be written as an EL equation where (5) with $D(q)$ represents the aircraft inertia matrix:

$$D(q) = \begin{bmatrix} I_x & 0 \\ 0 & I_z \end{bmatrix} = \begin{bmatrix} 40.07m & 0 \\ 0 & 99.92m \end{bmatrix}, \tag{7}$$

where I_x and I_z, are the aircraft inertia relative to the vehicle-carried axis in the x and z direction respectively. This aircraft has a nominal mass, m of 120 000 kg. The generalized coordinates are described by $q = [\phi\ \psi]^T$ and input, $u = [\delta_a\ \delta_r]^T$. Partial differential of the Rayleigh dissipation function is

$$\frac{\partial F}{\partial \dot{q}}(\dot{q}) = \begin{bmatrix} \frac{\partial F}{\partial \dot{\phi}} & \frac{\partial F}{\partial \dot{\psi}} \end{bmatrix}^T, \tag{8}$$

where

$\frac{\partial F}{\partial \dot{\phi}} = -1051.05\cos\theta\cos\psi(-1.4\beta + 6.6(-11\dot{\phi} + 11\dot{\psi}\sin\theta + 5\dot{\psi}\cos\phi\cos\theta - 5\dot{\theta}\sin\phi)/V_A)V_A^2 - 1051.05(\sin\phi\sin\theta\cos\psi - \cos\phi\sin\psi)(-0.4461 - 2.1505\alpha - 92.4424(\dot{\theta}\cos\phi + \dot{\psi}\sin\phi\cos\theta)/V_A + 0.11(6.0723\alpha + 1.0656 + 24.6016(\dot{\theta}\cos\phi + \dot{\psi}\sin\phi\cos\theta)/V_A)\cos(\alpha) + 0.11(0.13 + 0.07(5.5\alpha + 0.654)^2)\sin\alpha)V_A^2 - 1051.05(\cos\phi\sin\theta\cos\psi + \sin\phi\sin\psi)((1 - 3.819718633\alpha)\beta + 6.6(1.7\dot{\phi} - 1.7\dot{\psi}\sin\theta - 11.5\dot{\psi}\cos\phi\cos\theta + 11.5\dot{\theta}\sin\phi)/V_A - 0.176\beta)V_A^2$

and

$\frac{\partial F}{\partial \dot{\psi}} = 1051.05\sin\theta(-1.4\beta + 6.6(-11\dot{\phi} + 11\dot{\psi}\sin\theta + 5\dot{\psi}\cos\phi\cos\theta - 5\dot{\theta}\sin\phi)/V_A)V_A^2 - 1051.05\sin\phi\cos\theta(-0.4461 - 2.1504\alpha - 92.4424(\dot{\theta}\cos\phi + \dot{\psi}\sin\phi\cos\theta)/V_A + 0.11(6.0723\alpha + 1.0656 + 24.6016(\dot{\theta}\cos\phi + \dot{\psi}\sin\phi\cos\theta)/V_A)\cos\alpha + 0.11(0.13 + 0.07(5.5\alpha + 0.654)^2)\sin\alpha)V_A^2 - 1051.05\cos\phi\cos\theta((1 - 3.8197\alpha)\beta + 6.6(1.7\dot{\phi} - 1.7\dot{\psi}\sin\theta - 11.5\dot{\psi}\cos\phi\cos\theta + 11.5\dot{\theta}\sin\phi)/V_A - 0.176\beta)V_A^2$

The input matrix is

$$M_u = \begin{bmatrix} M_{\phi,\delta_a} & M_{\phi,\delta_r} \\ M_{\psi,\delta_a} & M_{\psi,\delta_r} \end{bmatrix}. \tag{9}$$

This input matrix is invertible since θ is fixed to 0.0284 rads for a level flight turn. The components of this input matrix are expressed in the following:

$M_{\phi,\delta_a} = -630.63V_A^2\cos\theta\cos\psi,$

$M_{\phi,\delta_r} = 231.231V_A^2\cos\theta\cos\psi - 634.41378V_A^2(\cos\phi\sin\theta\cos\psi + \sin\phi\sin\psi),$

$M_{\psi,\delta_a} = 630.63V_A^2\sin\theta,$

$M_{\psi,\delta_r} = -231.231V_A^2\sin\theta - 634.41378V_A^2\cos\phi\cos\theta.$

The Rayleigh dissipation function and the input matrix, M_u are due to drag, lift and sideforce contributions.

2.4 Controller design

Nonlinear Energy-Based tracking control technique is based on the passivity property of Euler-Lagrangian (EL) systems. The main focus of this paper is to present the design and implementation of NEM in an aircraft (lateral) control.

Let $\tilde{q} = q - q_r$, represents an error between the generalized coordinate, q and the corresponding desired value, q_r. We define an *error function* of the form

$$D(q)\ddot{\tilde{q}} + K_p\tilde{q} + K_d\dot{\tilde{q}} = \Psi, \tag{10}$$

where K_p and K_d are positive definite matrices. According to Ortega et al. [1998], this system defines an output strict passivity map $\Psi \mapsto \dot{\tilde{q}}$ with a storage function of

$$H(\dot{\tilde{q}}, \tilde{q}) = \frac{1}{2}\dot{\tilde{q}}^T D(q)\dot{\tilde{q}} + \frac{1}{2}\tilde{q}^T K_p \tilde{q}, \tag{11}$$

which is chosen based on a key *energy balance* established in (12) by integrating it from time 0 to time T.

$$\underbrace{H[q(T), \dot{q}(T)] - H[q(0), \dot{q}(0)]}_{stored energy} + \underbrace{\int_0^T \dot{q}^{\mathsf{T}} \frac{\partial F}{\partial \dot{q}}(\dot{q}) ds}_{dissipated} = \underbrace{\int_0^T \dot{q}^{\mathsf{T}} M_u u ds}_{supplied} \tag{12}$$

The Lyapunov Theorem and Invariant Set Theorem presented in Slotine and Li [1988] are applied to guarantee Global Asymptotic Stability for this control system.

Proposition 1. Consider the error function (10). If the control input in (13) is designed such that the storage function $H(\dot{\tilde{q}}, \tilde{q})$ is positive definite, $\dot{H}(\dot{\tilde{q}}, \tilde{q})$ is negative semi-definite, then the equilibrium point at 0 for error function in (10) is stable based on Lyapunov Theorem.

$$u = M_u^{-1}\left[D(q)\ddot{q}_r + \frac{\partial F}{\partial \dot{q}}(\dot{q}) - Q_\zeta - K_p\tilde{q} - K_d\dot{\tilde{q}}\right], \tag{13}$$

where $(.)_r$ denotes the desired reference value.

Proof: An appropriate storage function for the error function in (10) is given by $H(\tilde{q}, \tilde{q})$ in (11). Differentiating w.r.t. time gives (14).

$$\dot{H}(\dot{\tilde{q}}, \tilde{q}) = -\dot{\tilde{q}}^T K_d \dot{\tilde{q}} + \Psi^T \dot{\tilde{q}}, \tag{14}$$

Substituting (13) into (5) gives $\Psi = 0$ and therefore, (14) becomes

$$\dot{H}(\dot{\tilde{q}}, \tilde{q}) = -\dot{\tilde{q}}^T K_d \dot{\tilde{q}} \leq 0. \tag{15}$$

Let $\dot{\tilde{q}} = 0$ be the set of all points within a bounded region Ω where $\dot{H}(\dot{\tilde{q}}, \tilde{q}) = 0$, and $\tilde{q} = 0$ be the largest invariant set in $\dot{\tilde{q}} = 0$. Then based on the Global Invariant Set Theorem, every solution for $\tilde{q}$ originating in Ω converges to $\tilde{q} = 0$ as $t \to \infty$.

Further, the error function in (10) can be re-written as $\ddot{\tilde{q}} = -\frac{K_p \tilde{q}}{D(q)}$ which is equal to 0 *iff* $\tilde{q} = 0$, when $\dot{\tilde{q}} = 0$. This implies that the system will always converge to $\tilde{q} = 0$ and will remain at $[\tilde{q} = 0, \dot{\tilde{q}} = 0]$.

In addition, since $H(\dot{\tilde{q}}, \tilde{q})$ is unbounded as $\|\tilde{q}\| \to \infty$, the Ω region is unbounded. Thus, the equilibrium point at $[\tilde{q} = 0, \dot{\tilde{q}} = 0]$ is Globally Asymptotically Stable. In other words, $\tilde{q}$ and $\dot{\tilde{q}}$ is always converged to zero with this controller.

2.5 Tuning

The design constants, K_p and K_d, were tuned using the pole-placement technique based on a linearized model at the nominal operating condition, i.e. the aircraft is flying at an airspeed of 80 m/s and zero flight path angle, aircraft mass of 120,000 kg, and CoG (x_{cg}, y_{cg}, z_{cg}) of $(0.23, 0.0, 0.0)$. The design constants that satisfy the design criteria are:

Table 4. Simulation of 12 Flight Conditions

Simulation	Description
1	*Normal Operating Condition*
2	*Turbulence with constant wind of 10 m/s*
3	*Turbulence with constant wind of 20 m/s*
4	*Turbulence with constant wind of 30 m/s*
5	*Turbulence with constant wind of 40 m/s*
6	*Turbulence with constant wind of 50 m/s*
7	*Parameter change of m = 100000 kg*
8	*Parameter change of xcg = 0.15*
9	*Parameter change of ycg = −0.03*
10	*Parameter change of ycg = 0.03*
11	*Parameter change of zcg = 0.21*
12	*'Extreme' flight condition*

$$K_p = \begin{bmatrix} 739961492.4 & 0 \\ 0 & 18628496.21 \end{bmatrix}$$

and

$$K_d = \begin{bmatrix} 178080521.8 & 0 \\ 0 & 14963747.96 \end{bmatrix}$$

The magnitude of these design constants are quite large. This is as expected because the order of magnitude of these terms have to be equivalent to those in (7) which takes its value from the aircraft inertia that is very large.

3. DISTURBANCE REJECTION AND ROBUSTNESS ANALYSIS

In this section we provide a robustness analysis based on twelve sets of simulations that represent various flight conditions. The closed-loop responses of the NEM controller are compared with a LQR (with integral action) controller as a typical example.

3.1 Flight condition

The aircraft in Simulation 1 operates at normal operating conditions without any wind disturbances. Simulation 2 to 6 includes wind turbulences and constant side wind of 10 m/s to 50 m/s. The wind model is activated throughout the entire 100 seconds with a turbulence generated based on von Karman model superimposed by a constant cross-wind of 10 m/s. Djurovic et al. [2000] explains the application of the von Karman turbulence model. Some parameters of the aircraft such as the location of center of gravity, CoG, and mass of the aircraft, m, are varied in Simulation 7 to 11. Finally, a combination of wind turbulences and constant wind of 50 m/s together with a shifted position of the CoG in three different major axis (xcg=0.15, ycg=-0.03 and zcg=0.21) of the aircraft body reference frame tests the controllers with an 'extreme' flight condition in Simulation 12. Details of all 12 simulations are summarized in Table 4.

These parameter changes implemented are in line with evaluation procedures given in FM [AG08].

3.2 Simulation Results at Normal Operating Condition (Simulation 1)

A roll angle of approximately 23^o is required for the RCAM to achieve a turn rate of $3^o/s$ as described in Looye and

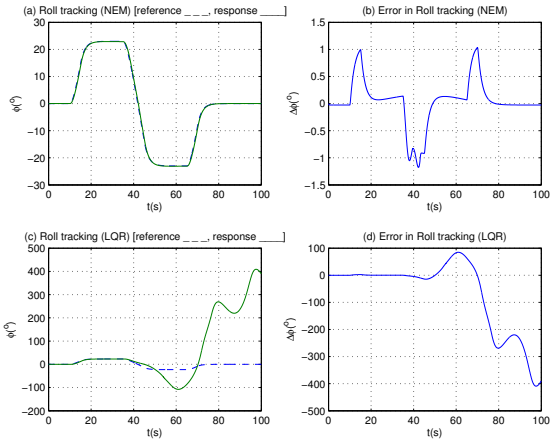

Fig. 2. Rolling angle response at normal operating condition (Simulation 1)

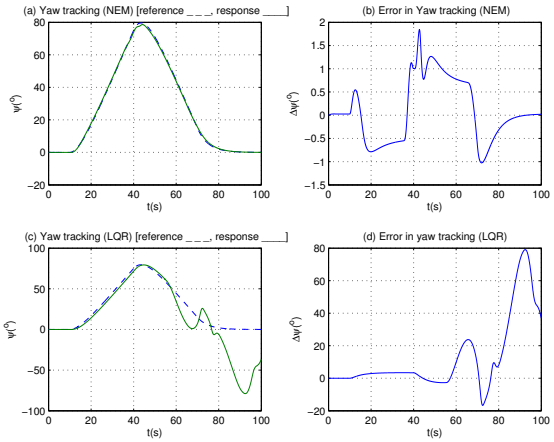

Fig. 3. Yawing angle at normal operating condition (Simulation 1)

Bennani [4 April 1997]. A positive roll angle will result in a positive yaw angle. Fig. 2(a) shows the response of roll angle with the NEM controller. This NEM controller is able to track the reference roll angle throughout the entire simulation time with less than 1^o steady state error, which is less than the maximum allowable steady state error of 5^o specified by the performance criteria as shown in Fig. 2(b). On the other hand, the LQR controller becomes unstable and fails to track roll command after 35 seconds as the aircraft is operating at different trim condition, as seen in Fig. 2 (c) and (d). This is consistent with the fact that the LQR controller fails to track both roll and yaw commands along the second part of the simulation is that the controllers have reached their saturation limits as seen in Fig. 4(c) and (d).

The yaw command is tracked by the NEM controller with no overshoot. Fig. 3(a) gives a complete picture of the NEM controler tracking the reference yaw. There is minimal steady state error in yaw tracking as seen in Fig. 3(b). At 65 seconds, the LQR controller fails to track yaw command, shown in Fig. 3(c) and (d).

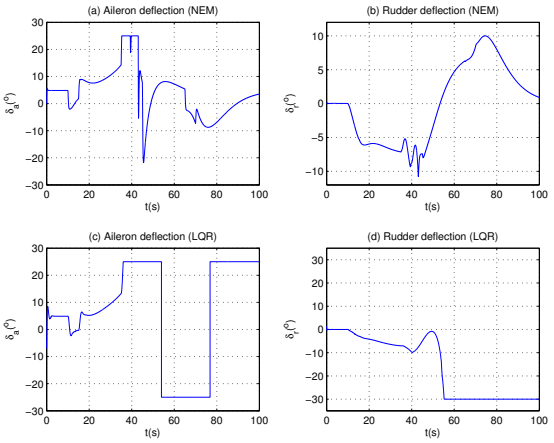

Fig. 4. Aileron and rudder inputs at normal operating condition (Simulation 1)

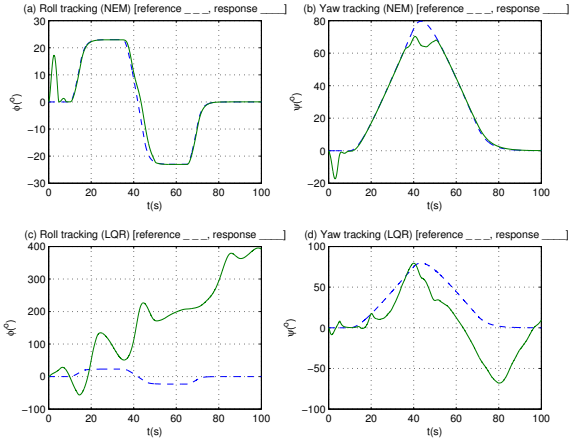

Fig. 5. Roll and Yaw Tracking at 'extreme' flight condition (Simulation 12)

Comparing the aileron and rudder deflections, both the aileron and rudder are only allowed to function within a saturated limit of $\pm 25^o$ and $\pm 30^o$ respectively. The aileron and rudder deflection controlled by the NEM controller are shown in Fig. 4(a) and (b). The observation shows that the NEM controller is capable of distributing energy provided by thrust into roll and yaw dynamics more appropriately, which reduces the possibility of reaching their saturation limits.

3.3 Simulation Results at 'Extreme' Operating Condition (Simulation 12)

Both controllers are tested with wind disturbances and parameter changes such as aircraft mass and a shifted CoG of the aircraft. This condition is said to be extreme because the aircraft is operating much higher than the criteria defined by GARTEUR as moderate. See FM [AG08]. Simulation results in Fig. 5 shows that the NEM controller is capable of providing stability and performance robustness despite the extreme flight condition as compared to the LQR controller which has very bad tracking right from the start of simulation.

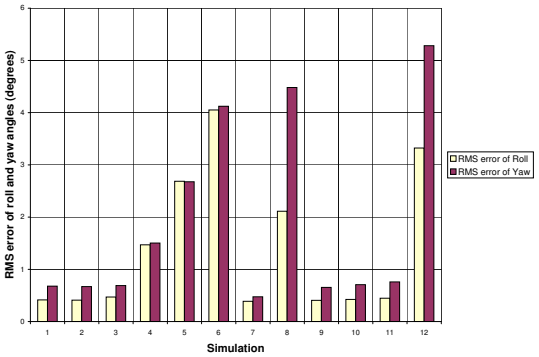

Fig. 6. Root-mean-square errors of roll and yaw angles for NEM controller

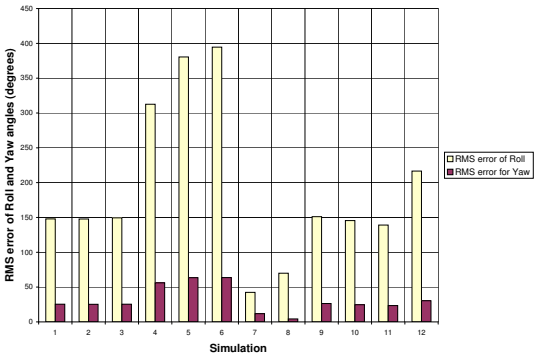

Fig. 7. Root-mean-square errors of roll and yaw angles for LQR controller

3.4 Summary of other Flight Conditions (Simulation 2-11)

Other simulation test shown in Simulation 2 to 11 were implemented with less extreme conditions and wind disturbances. The root-mean-square (RMS) error of roll and yaw angles are summarized in Fig. 6 and 7 for the NEM and LQR controllers respectively.

Both roll and yaw command were tracked within 5^o RMS error using the NEM controller except for Simulation 12. However, all responses with the NEM controller are well within the safety criteria of keeping the roll angle errors to less than 30^o whereas the LQR controller was unable to keep the roll angle errors within the specified criteria. The yaw angle RMS error of the LQR controller were up to 15.5 times higher than the NEM controller at Simulation 6.

4. CONCLUSION

The proposed NEM controller for lateral control has successfully been designed and tested against various flight conditions. The results show that the NEM controller has better performance, robustness and disturbance rejection to track commanded roll and yaw angles. As a comparison we have shown that the closed-loop responses of the aircraft with NEM are far better than those with an LQR controller (with integral action). Further study is required to include the 'slow' lateral dynamics such as the sideslip motion and positional tracking. Further study is also required to design a complete controller that consist of NEM controller(s) for a complete and integrated longitudinal and lateral dynamics to track a particular trajectory or path in a 3-dimensional space.

REFERENCES

Rini Akmeliawati. Nonlinear control for automatic flight control systems. *PhD thesis, University of Melbourne*, 2001.

Rini Akmeliawati and Iven Mareels. Flight control systems using passivity-based control - disturbance rejection and robustness analysis. *AIAA Guidance, Navigation, and Control Conference and Exhibit*, 2, 1999.

Rini Akmeliawati and Iven Mareels. Nonlinear energy-based control method for aircraft dynamics. *Proceedings of the 40th IEEE Conference on Decision and Control*, 658-663, 2001.

Zeljko Djurovic, Ljubisa Miskovic, and Branko Kovacevic. Simulation of air turbulence signal and its application. *Proceedings of the 10th Mediterranean Electrotechnical Conference*, 2:847–850, 2000.

FM(AG08). Robust flight control design challenge problem formulation and manual: the research civil aircraft model (RCAM). *Technical Report GARTEUR/TP-088-3, GARTEUR*, 17 February 1997.

John Griswold. Integrated flight and propulsion control system design for a business jet. *Proceedings of AIAA Guidance, Control and Navigation Conference and Exhibition*, 2000-4542:1–8, 2000.

R. A. Hyde. An h_∞ loop-shaping design for the vaac harrier. *In R. W. Pratt, editor, Flight Control Systems, Practical Issues in Design and Implementation*, -:348–373, 2000.

A. A. Lambregts. Automatic flight controls concepts and methods. *FAA National Resource Specialist Advanced Controls*, pages 1–22, 1998.

Gertjan Looye and Samir Bennani. Description and analysis of the research civil aircraft model (RCAM). *Technical Report GARTEUR/TP-088-27, GARTEUR*, 4 April 1997.

R. Ortega, A. Loria, P. J. Nicklasson, and H. Sira-Ramirez. *Passivity-based Control of Euler-Lagrange Systems: Mechanical, Electrical and Electromechanical Applications*. Springer-Verlag London Limited, 1998.

Jean-Jacques E. Slotine and Weiping Li. Adaptive manipulator control: a case study. *IEEE Trans. on Automat. Contr.*, 33:995–1003, 1988.

Puneet Wahi, Ravi Raina, and Fahmida N. Chowdhury. A survey of recent work in adaptive flight control. *Proceedings of the 33rd Southeastern Symposium on System Theory*, 74:7–12, 18-20 March 2001.